Supporting Information

Halogenated Dibenzoylmethane Eu^{3+} Complexes as Spectroscopic Markers: Pioneering Photobleaching Strategy for Counterfeit Applications and Control of Luminescence Efficiency

Alisia V. Tsorieva[a*], Vladislav M. Korshunov[a], Mikhail T. Metlin[a], Tatiana S. Vlasova[b], Victoria E. Gontcharenko[a,c], Daria A. Metlina[a], Victor O. Kompanets [d], Sergey V. Chekalin [d] and Ilya V. Taydakov[a*]

[a] P.N. Lebedev Physical Institute of the Russian Academy of Sciences, 53 Leninskiy 1. Prospect, 119991 Moscow, Russia

[b] Mendeleev University of Chemical Technology, Miusskaya Ploshchad', 125047 9, Moscow, Russia

[c] Faculty of Chemistry, National Research University Higher School of Economics, 20 Miasnitskaya Street, 101000 Moscow, Russia

[d] Institute of Spectroscopy of the Russian Academy of Sciences, 5 Fizicheskaya Ul., Moscow, 108840, Russia

E-mails: tsorievaav@gmail.com, taidakov@gmail.com

Table of contents:

SI-1. Methods and materials

SI-1.1. Synthesis of ligands and complexes

All common reagents were purchased from Aldrich or Acros Organics and were used without further purification. THF was distilled over Na/benzophenone under Ar atmosphere before use. DMSO was distilled at 20 torr over CaH_2 and stored over 3A molecular sieves. Reaction with NaH were conducted in dry Ar atmosphere.

Elemental analysis was performed on the Elementar CHNO(S) analyzer (Elementar Analysensysteme GmbH, Langenselbold, Germany). Samarium content was determinated by complexometric titration by standard Trilon B (Disodium dihydrogen ethylenediaminetetraacetate) solution in the presence of Xylenol Orange as an indicator. Sample was decompose by heating with 70% HNO_3 before titration. ^1H and ^{13}C-NMR spectra were acquired using a Bruker AV-300 instrument operated at 300 and 75.5 MHz, respectively, in DMSO-*d6* or $CDCl_3$ solutions and reported relatively TMS (δ = 0.00 ppm)

Bis(4-iodophenyl)propane-1.3-dione (HIDBM)

Sodium hydride (60 % dispersion in mineral oil, 0.7 g, 17.5 mmol) was washed by dry hexane (3 portions of 50 mL) to remove an oil and suspended under vigorous magnetic stirring in THF (15 mL). The resulted suspension was cooled in an ice bath to +5 C. Separately methyl 4-iodobenzoate (4.42 g, 16.9 mmol) and 4-iodoacetopenone (4.15 g, 16.9 mmol) were dissolved in mixture of 25 mL THF and 5 mL DMSO. The resulted solution was added dropwise to stirred NaH suspension with continuous cooling and resulted orange mixture was stirred at a room temperature for 6 h. The reaction was quenched by carefully addition of 1.3 mL of 35 % HCl and THF was removed by vacuum evaporation. The resulted solution was poured into MeOH (100 mL) with stirring. Precipitated diketone was collected, washed by 10mL of MeOH and recrystallized from hot EtOAc, afforded pure diketone as yellowish crystalline powder.

Yield was 4.6 g (57%). Light yellow powder. ^1H-NMR (DMSO-d_6, ppm), δ = 7.95 (m, 8H), 7.35 (s, 1H, CH of enolic form). ^{13}C-NMR (DMSO-d_6, ppm): δ = 184.58, 137.77, 133.88, 129.13, 101.54, 93.28.

General method for preparation bis(4-halophenyl)propane-1.3-diones (HFDBM, HClDBM and HBrDBM)

Sodium hydride (60 % dispersion in mineral oil, 3.0 g, 75 mmol) was washed by dry hexane (3 portions of 50 mL) to remove an oil and suspended under vigorous magnetic stirring in THF (100 mL). At 0- (+5) ˚C 50 mmol of corresponding ethyl 4-halobenzoate, dissolved in 20 ml of

THF, followed by a solution of 48 mmol of corresponding 4-haloacetophenone in 50 mL of THF was added slowly. In case of 4-chloro- or bromoacetophenone 20 mL of DMSO was added to THF to dissolve ketone completely. The reaction mixture was stirred in a cooling bath for 1h and 6 h at a room temperature. The reaction mixture was evaporated to a half of initial volume on rotary evaporator and poured on 250 g of crushed ice mixed with 5.5 mL of conc. HCl. The precipitate of diketone was separated, dissolved in CH_2Cl_2 (100-500mL) and organic solution was washed successively by 50 mL of water and 50mL of brine. Organic phase was separated, dried over $MgSO_4$ and evaporated to dryness. The resulted solid diketone was recrystallized from EtOH or hexane-CH_2Cl_2 mixture.

Bis(4-fluorophenyl)propane-1.3-dione (HFDBM)

Yield was 6.9 g (52%). White solid. ^{1}H-NMR ($CDCl_3$, ppm), δ = 9.58 (s, 1H), 8.11 (d, J = 3.2 Hz, 4 H), 7.17 (d, J = 8.8 Hz, 4 H), 6.73 (s, 1 H). ^{13}C-NMR ($CDCl_3$, ppm): δ = 184.61, 165.63 (d, J = 252.6 Hz), 131.82 (d, J = 3.0 Hz),129.79 (d, J = 9.1 Hz, 1C), 116.06 (d, J = 21.8 Hz, 1C), 92.63. ^{19}F-NMR (282.4 MHz, $CDCl_3$, ppm): δ = -104.91 (rel. $CFCl_3$, δ =0.00 ppm)

Bis(4-chlorophenyl)propane-1.3-dione (HClDBM)

Yield was 10.2 g (70%). Yellow solid. ^{1}H-NMR ($CDCl_3$, ppm), δ = 16.74 (s, 1H), 7.93 (d, J = 7.8 Hz, 4 H), 7.47 (d, J = 8.4 Hz, 4 H), 6.76 (s, 1 H). ^{13}C-NMR ($CDCl_3$, ppm): δ = 184.71, 139.01, 133.89, 129.27, 128.63, 93.00.

Bis(4-bromophenyl)propane-1.3-dione (HBrDBM)

Yield was 11.9 g (63%). Yellowish solid. ^{1}H-NMR ($CDCl_3$, ppm), δ = 16.73 (s, 1H), 7.85(d, J = 7.2 Hz, 4 H), 7.63 (d, J = 8.4 Hz, 4 H), 6.78 (s, 1 H). ^{13}C-NMR ($CDCl_3$, ppm): δ = 184.73, 139.03, 133.91, 129.30, 128.61, 93.00.

General method for preparation of complexes [$Eu(L)_3(phen)$].

To a warm (45° C) solution of diketone (0.6 mmol) in 20 mL of MeOH-THF mixture (1/2 by vol.) 1M methanolic NaOH solution (0.6 mL, 0.6 mmol) was added slowly with stirring and resulted mixture was left for 10 min. Then solution of 1.10-phenanthroline (36 mg, 0.2mmol) in 5 mL of THF was added, followed by slow addition of hot $EuCl_3 \cdot 6H_2O$ solution (73 mg, 0.2 mmol) in 1 mL of MeOH. The resulted suspension was stirred in a closed vial at 45° C for 3 h and cooled to a room temperature. Precipitate of complex was separated, washed successively by 5 mL of MeOH, 5 mL of 30 % aqueous MeOH solution, 5mL of distilled water and 10 mL of hexane. Solid was dried at 0.1 torr to a constant weight and purified by recrystallization from MeOH – $CHCl_3$ mixture.

[$Eu(FDBM)_3(phen)$]

Light yellow powder. Yield is 0.140 g (63%). Anal. calcd. for $C_{57}H_{35}EuF_6N_2O_6$ (FW1109.85): C, 61.68; H, 3.18; N, 2.52; Eu, 13.69%. Found: C, 61.73; H, 3.15; N, 2.58; Eu, 13.81%.

[Eu(ClDBM)$_3$(phen)]

Light yellow powder. Yield is 0.182 g (75%). Anal. calcd. for $C_{57}H_{35}Cl_6EuN_2O_6$ (FW1208.51): C, 56.65; H, 2.92; N, 2.32; Eu, 12.57 %. Found: C, 56.72; H, 3.01; N, 2.382; Eu, 12.79%.

[Eu(BrDBM)$_3$(phen)]

Light yellow powder. Yield is 0.239 g (81%). Anal. calcd. for $C_{57}H_{35}Br_6EuN_2O_6$ (FW1475.28): C, 46.41; H, 2.39; N, 1.90; Eu, 10.30 %. Found: C, 46.56; H, 2.44; N, 1.81; Eu, 10.44 %.

[Eu(IDBM)$_3$(phen)]

Light yellow powder. Yield is 0.239 g (81%). Anal. calcd. for $C_{57}H_{35}EuI_6N_2O_6$ (FW1757.28): C, 38.96; H, 2.01; N, 1.59; Eu, 8.56 %. Found: C, 39.02; H, 2.08; N, 1.66; Eu, 8.73 %.

General method for preparation of complexes $[Eu(L)_3(H_2O)_2]$, $[Gd(L)_3(H_2O)_2]$ and $[Tb(L)_3(H_2O)_2]$

To a warm (45° C) solution of diketone (0.6 mmol) in 20 mL of MeOH-THF mixture (1/2 by vol.) 1M methanolic NaOH solution (0.6 mL, 0.6 mmol) was added slowly with stirring and resulted mixture was left for 10 min. Then hot solution of $EuCl_3{\cdot}6H_2O$ (73 mg, 0.2 mmol), GdCl3$\cdot 6H_2O$ (74 mg, 0.2 mmol) or $TbCl_3{\cdot}6H_2O$ (75 mg, 0.2 mmol) in 1 mL of MeOH was added dropwise. The resulted suspension was stirred in a closed vial at 45° C for 3 h and cooled to a room temperature. Distilled water (3 mL) was added with vigorous stirring and solution was left in an open vial at a room temperature for 2 days. During this period of time, the solution evaporated slowly to ½ of its initial volume and precipitate formed. The crystalline product was filtered, washed successively by 5 mL of 30 % aqueous MeOH solution, 5mL of distilled water and 10 mL of hexane. Solid was dried at 0.1 torr to a constant weight.

[Eu(FDBM)$_3$(H$_2$O)$_2$]

Yellow powder. Yield is 0.083 g (43%). Anal. calcd. for $C_{45}H_{31}EuF_6O_8$ (FW965.67): C, 55.97; H, 3.24; Eu, 15.74 %. Found: C, 56.04; H, 3.29; Eu, 16.01 %.

[Gd(FDBM)$_3$(H$_2$O)$_2$]

Yellow powder. Yield is 0.093 g (48%). Anal. calcd. for $C_{45}H_{31}F_6GdO_8$ (FW970.96): C, 55.66; H, 3.22; Gd, 16.20 %. Found: C, 55.71; H, 3.29; Gd, 16.38 %.

[Tb(FDBM)$_3$(H$_2$O)$_2$]

Light yellow powder. Yield is 0.115 g (59%). Anal. calcd. for $C_{45}H_{31}F_6O_8Tb$ (FW972.64): C, 55.57; H, 3.21; Tb, 16.34%. Found: C, 55.49; H, 3.32; Tb, 16.46%

[Eu(ClDBM)$_3$(H$_2$O)$_2$]

Yellow powder. Yield is 0.125 g (59%). Anal. calcd. for $C_{45}H_{31}Cl_6EuO_8$ (FW1064.40): C, 50.78; H, 2.94; Eu, 14.28%. Found: C, 50.87; H, 2.99; Eu, 14.36%

[Gd(ClDBM)$_3$(H$_2$O)$_2$]

Yellow powder. Yield is 0.116 g (54%). Anal. calcd. for $C_{45}H_{31}Cl_6GdO_8$ (FW1069.69): C, 50.53; H, 2.92; Gd, 14.70%. Found: C, 50.61; H, 3.06; Gd, 14.97%.

[Tb(ClDBM)$_3$(H$_2$O)$_2$]

Light yellow powder. Yield is 0.103 g (48%). Anal. calcd. for $C_{45}H_{31}Cl_6O_8Tb$ (FW1071.36): C, 50.45; H, 2.92; Tb, 14.83%. Found: C, 50.57; H, 2.99; Tb, 15.02%.

[Eu(BrDBM)$_3$(H$_2$O)$_2$]

Yellow powder. Yield is 0.157 g (59%). Anal. calcd. for $C_{45}H_{31}Br_6EuO_8$ (FW1331.12): C, 40.60; H, 2.35; Eu, 11.42%. Found: C, 40.69; H, 2.41; Eu, 11.66%.

[Gd(BrDBM)$_3$(H$_2$O)$_2$]

Yellow powder. Yield is 0.168 g (63%). Anal. calcd. for $C_{45}H_{31}Br_6GdO_8$ (FW1336.40): C, 40.44; H, 2.34; Gd, 11.77%. Found: C, 40.53; H, 2.29; Gd, 11.89%.

[Tb(BrDBM)$_3$(H$_2$O)$_2$]

Light yellow powder. Yield is 0.160 g (60%). Anal. calcd. for $C_{45}H_{31}Br_6O_8Tb$ (FW1338.07): C, 40.39; H, 2.34; Tb, 11.88%. Found: C, 40.48; H, 2.39; Tb, 12.04%.

[Eu(IDBM)$_3$(H$_2$O)$_2$]

Yellow powder. Yield is 0.157 g (59%). Anal. calcd. for $C_{45}H_{31}EuI_6O_8$ (FW1613.11): C, 33.51; H, 1.94; Eu, 9.42%. Found: C, 33.67; H, 1.99; Eu, 9.58%.

[Gd(IDBM)$_3$(H$_2$O)$_2$]

Yellow powder. Yield is 0.217 g (67%). Anal. calcd. for $C_{45}H_{31}GdI_6O_8$ (FW1618.40): C, 33.40; H, 1.93; Gd, 9.72%. Found: C, 33.47; H, 2.01; Gd, 9.94%.

[Tb(IDBM)$_3$(H$_2$O)$_2$]

Light yellow powder. Yield is 0.139 g (43%). Anal. calcd. for $C_{45}H_{31}I_6O_8Tb$ (FW1620.07): C, 33.36; H, 1.93; Tb, 9.81%. Found: C, 33.40; H, 1.99; Tb, 9.97%.

SI-1.2. Single crystal and powder X- ray diffraction measurements

Single-crystal X-ray diffraction (SCXRD) analysis of ***Eu-FDBM-p, Eu-ClDBM-p. Eu-BrDBM-p*** and ***Eu-IDBM-p*** compounds was carried out on a Bruker D8 Quest diffractometer (MoKα radiation, ω and φ-scan mode). The structures were solved with direct methods and refined by least-squares method in the full-matrix anisotropic approximation on F^2. All hydrogen atoms were located in calculated positions and refined within riding model. In

Eu-FDBM-p, the positional disorder of the solvent chloroform molecule is present with site occupancies of 0.55/0.45. All calculations were performed using the SHELXTL and Olex2 software packages.[1,2] Atomic coordinates, bond lengths, angles, and thermal parameters have been deposited at the Cambridge Crystallographic Data Centre with deposition numbers — CCDC 2301532-2301534, 2301538, which are available free of charge at www.ccdc.cam.ac.uk.

Powder X-ray diffraction (PXRD) patterns were measured on D/MAX 2500 (Rigaku Corporation, Tokyo, Japan) diffractometer in the reflection mode with CuKα1 radiation (λ = 1.54056 Å) and curved graphite [002] monochromator placed in the reflected beam.

SI-1.3. Photophysical measurements

UV–Vis spectra of investigated compounds dissolved in tetrahydrofuran (HPLC SuperGradient, Panreac, Spain) were recorded with a JASCO V-770 spectrophotometer operating within 200–2500 nm. The concentration of the solutions was about 10^{-5} M. The measurements were performed using quartz cells with a 1 cm path length.

Excitation spectra and photoluminescence spectra were obtained using a Horiba Fluorolog QM spectrofluorimeter with a 75 W xenon arc lamp as excitation source and a R13456 (Hamamatsu, Japan) photomultiplier tube sensitive in the 200-980 nm emission range as a detector.

The photoluminescence quantum yields were measured for solid samples by an absolute method using the same experimental setup equipped with a G8 (GMP, Switzerland) integration sphere.

Luminescence decays were measured by Multichannel Scaling (MCS) method. For this purpose pulsed laser radiation of Nd:YAG laser LQ529B (Solar LS, Belarus) with repetition rate 20 Hz and pulse duration 8 ns was used. The excitation wavelength was selected using system based on optical parametric oscillator (OPO) LP604 and second harmonic generator LG350 (Solar LS, Belarus) pumped by second harmonic (532 nm) of LQ529B. The setup provides continuous tuning of laser wavelength in the range 340-2500 nm. The data were obtained on the Horiba Fluorolog QM spectrofluorimeter.

The temperature stimulated luminescence (TSL) measurements were recorded with a special in-house made setup. Complexes sandwiched between two quartz slides were placed inside a vacuum optical cryostat LN-121-SPECTR (Cryotrade, Russia) cooled with liquid nitrogen. The residual pressure was below 10^{-5} torr. The temperature of the sample was measured by a resistive wire sensor connected to a LakeShore 325 temperature controller placed on a copper sample holder inside the cryostat in close proximity to the sample. The temperature in the range

of 78–300 K was maintained by a special heater that was mounted on the sample holder and controlled by the same temperature controller. Cryostat was placed into the Horiba Fluorolog QM spectrofluorimeter.

SI-1.4. Transient absorption measurements

For the transient absorption (TA) experiments, MeOH solutions of the complexes with an optical density of about 0.2 were prepared. To avoid photodegradation, solutions were poured into a 1-mm-thick rotating cell. TA spectra were measured on an ultrafast spectrometer based on an optical parametric amplifier (TOPAS, Light Conversion) pumped at 800~nm by a Ti:Sa femtosecond regenerative amplifier (Spitfire HP, Spectra Physics). The TA measurements were performed with optical excitation of the ligands in complexes. For this purpose, laser pulses at 380 nm with a 1 kHz repetition rate and duration of about 100 fs were used. A part of the laser beam from the output of the regenerative amplifier was focused into a water cell to generate white-light continuum for broadband probing of the absorption changes. The instrument response function recorded for MeOH solvent has a characteristic time scale of 200 fs.
Threshold irradiation power density was measured by COHERENT Field Max II.

SI-1.5. Electron scanning microscopy (SEM)

Target-oriented approach was utilized for the optimization of the analytic measurements.[3] Before measurements the samples were mounted on a 25 mm aluminum specimen stub, fixed by conductive carbon tape. Metal coating with a thin film (6 nm) of Au/Pd was performed using magnetron sputtering method as described earlier and coated with a 20 nm film of carbon.[4] The observations were carried out using Hitachi Regulus8230 field-emission scanning electron microscope (FE-SEM). Images were acquired in backscattered electron mode (compositional contrast) at a 20 kV accelerating voltage and in secondary electron mode at 1 kV accelerating voltage. EDS-SEM studies were carried out using Bruker Quantax 400 EDS system equipped with XFlash 6|60 detector at a 20 kV accelerating voltage.

SI-2. Results and discussion

SI-2.1. Discussion on synthesis

There are only few papers utilizing well-known dibenzoylmethane bearing halogen atoms in the position *C(4)* of both benzene rings as ligands for preparation of complexes.

Thus, complexes of boron,[5] iridium(III), iron (III), cobalt (III), copper(II), platinum (IV),[6] tungsten(VI),[7] ruthenium (II) and nickel (II) were described.[8-14] Complexes with selected lanthanides and different ancillary ligands were also synthesized, but luminescent properties of such complexes were not systematically investigated up to date.[15-20]

Halogenated dibenzoylmethanes were obtained previously by several methods – Claisen condensation of corresponding substituted 4-halogenacetophenones and 4-halogenbenzoates, by interaction of 4-halogenanated benzoyl chlorides with vinyl acetate in the presence of $AlCl_3$, by acylation of 4-halogenacetophenones enolates by 4-halogenanated benzoyl chlorides and by chalcone bromination-debromination sequence.[15,21-29]

We have found the method developed by W. Franek is the most suitable for the preparation of all four diketones.[26] In this method, DMSO-THF mixture was used as a solvent in combination with NaH as a base. Due to low solubility of iodinated diketone, sodium enolate in pure THF DMSO addition is mandatory in this reaction, but it may be omitted for preparation of other halogenated diketones (**Scheme S1**).

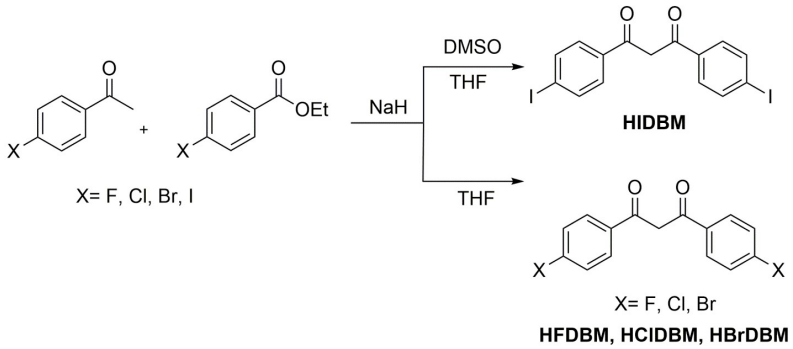

Scheme S1. Synthesis of 4-halogenated dibenzoylmethanes.

Complexes with Eu^{3+} and Gd^{3+} ions were synthesized in a conventional manner by interaction of free diketone, NaOH and corresponding hydrated lanthanide chloride in the molar ratio 3:3:1. Methanol-THF mixture was used as a solvent due to low solubility of ***HBrDBM*** and ***HIDBM*** ligands (Scheme 1). Hydrated complexes of composition $[Eu(L)_3(H_2O)_2]$ and $[Gd(L)_3(H_2O)_2]$ were precipitated by slowly adding distilled water to the reaction mixture. For preparation of complexes with 1.10-phenanthroline (***Phen***), this ligand was added to the solution of sodium salt of diketone before addition of metal chloride solution. Complexes of composition $[Eu(L)_3(phen)]$ were separated upon slow evaporation of reaction mixture. They were additionally purified by recrystallization from $CHCl_3$ and $MeOH/CHCl_3$ mixtures.

SI-2.2. Crystal structures and powder X-ray diffraction (PXRD) data

Table S1. Crystal data and refinement parameters for ***Eu-FDBM-p, Eu-ClDBM-p, Eu-BrDBM-p, Eu-IDBM-p***.

Parameter	Value			
	Eu-FDBM-p	***Eu-ClDBM-p***	***Eu-BrDBM-p***	***Eu-IDBM-p***
Molecular Formulae	$C_{57}H_{35}EuF_6N_2O_6$, $CHCl_3$	$C_{57}H_{35}EuCl_6N_2O_6$	$C_{57}H_{35}EuBr_6N_2O_6$	$C_{57}H_{35}EuI_6N_2O_6$
M	1229.20	1208.53	1475.29	1757.23
T, K	110(2)	110(2)	110(2)	110(2)
System	Triclinic	Monoclinic	Monoclinic	Monoclinic
Space group	*P-1*	$P2_1/n$	$P2_1/n$	$P2_1/n$
a, Å	12.7998(4)	14.1895(14)	14.4348(17)	15.002(2)
b, Å	12.8604(4)	18.0974(18)	18.382(2)	18.604(3)
c, Å	16.3328(5)	20.0737(19)	20.131(2)	20.390(3)
α, deg.	98.3270(10)	90	90	90
β, deg.	94.9730(10)	94.015(3)	94.856(6)	94.521(5)
γ, deg.	109.7010(10)	90	90	90
V, Å^3	2477.85(13)	5142.1(9)	5322.3(10)	5673.0(14)
Z	2	4	4	4
ρ_{calc}, g cm^{-3}	1.648	1.561	1.841	2.057
$\mu(MoK_\alpha)$, mm^{-1}	1.507	1.585	5.735	4.420
F(000)	1228	2416	2848	3280
θmin–θmax, deg	1.71 – 29.00	1.70 – 29.00	1.503 – 26.000	1.63 – 30.56
Number of measured reflections	37485	50402	40618	62949
Number of unique reflections (R_{int})	13171 (0.0685)	13681 (0.0804)	10452 (0.0996)	17347 (0.0684)
Number of reflections with $I > 2\sigma(I)$	10853	10763	7974	12997
Number of refined	694	649	649	649

parameters				
R-factors ($I > 2\sigma(I)$)	R_1 = 0.0411, ωR_2 = 0.0834	R_1 = 0.0453, ωR_2 = 0.0906	R_1 = 0.0419, ωR_2 = 0.0949	R_1 = 0.0391, ωR_2 = 0.0715
R-factors (all reflections)	R_1 = 0.0567, ωR_2 = 0.0884	R_1 = 0.0614, ωR_2 = 0.0989	R_1 = 0.0626, ωR_2 = 0.1057	R_1 = 0.0630, ωR_2 = 0.0784
GOOF	1.051	1.025	0.970	1.028
$\Delta\rho_{max}$ / $\Delta\rho_{min}$, e/Å^3	1.235 / -1.620	1.121 / -1.524	1.117 / -0.623	1.800 / -1.718

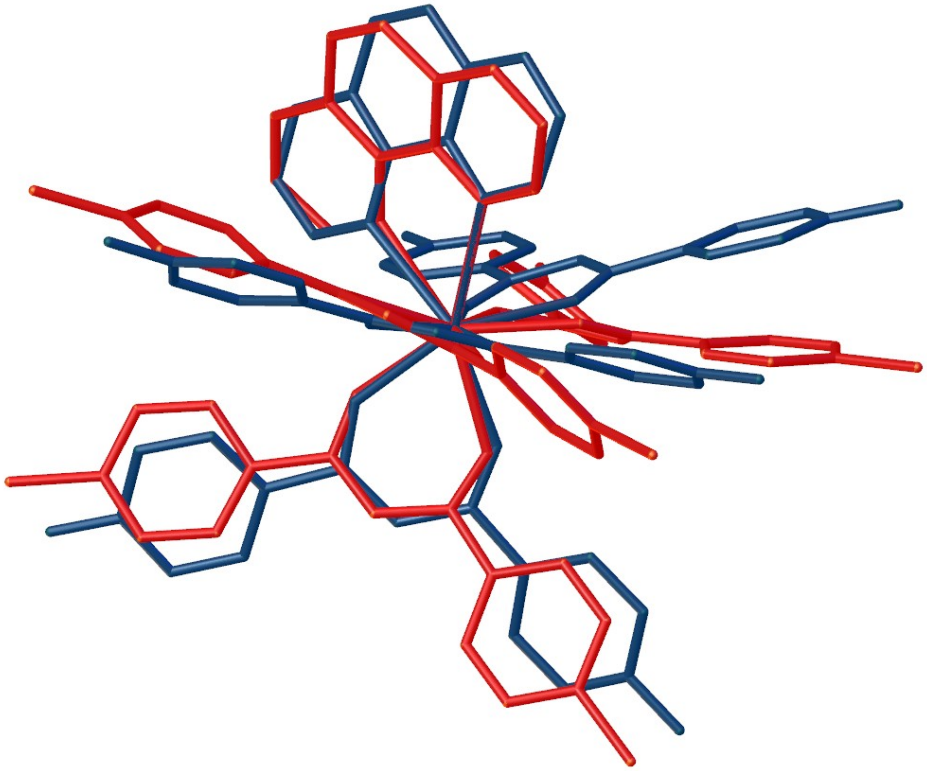

Figure S1. View of the overlayed ***Eu-FDBM-p*** and ***Eu-ClDBM-p*** complex molecules (drawn in red and blue, respectively). Thermal ellipsoids of atomic displacement are not shown, hydrogen atoms are omitted for clarity.

Table S2. Bond lengths of Eu^{3+} coordination environment in corresponding complexes.

Eu1-X bond length, Å	***Eu-FDBM-p***	***Eu-ClDBM-p***	***Eu-BrDBM-p***	***Eu-IDBM-p***
Eu1-O1	*2.356(2)*	*2.355(2)*	*2.350(3)*	*2.325(3)*
Eu1-O2	*2.347(2)*	*2.318(2)*	*2.322(3)*	*2.342(3)*

Eu1-O3	*2.359(2)*	*2.325(2)*	*2.314(3)*	*2.365(3)*
Eu1-O4	*2.323(2)*	*2.370(2)*	*2.367(3)*	*2.324(3)*
Eu1-O5	*2.370(2)*	*2.345(2)*	*2.346(3)*	*2.347(3)*
Eu1-O6	*2.330(2)*	*2.327(2)*	*2.340(3)*	*2.340(3)*
Eu1-N1	*2.598(3)*	*2.615(3)*	*2.618(4)*	*2.600(3)*
Eu1-N2	*2.638(3)*	*2.597(3)*	*2.604(4)*	*2.633(3)*
Mean Eu1-O bond length, Å	***2.347(2)***	***2.340(2)***	***2.340(3)***	***2.340(3)***

Table S3. *C-O* and *C-C* bond lengths in diketone ligands in corresponding complexes.

Bond length, Å	***Eu-FDBM-p***	***Eu-ClDBM-p***	***Eu-BrDBM-p***	***Eu-IDBM-p***
C1-O1	*1.258(3)*	*1.272(4)*	*1.272(6)*	*1.260(4)*
C3-O2	*1.269(3)*	*1.268(4)*	*1.263(5)*	*1.267(4)*
|ΔC-O|	*0.011(6)*	*0.004(8)*	*0.009(11)*	*0.007(8)*
C1-C2	*1.404(4)*	*1.407(4)*	*1.403(7)*	*1.398(5)*
C2-C3	*1.394(4)*	*1.405(4)*	*1.402(7)*	*1.419(5)*
|ΔC-C|	*0.010(8)*	*0.002(8)*	*0.001(14)*	*0.021(10)*
C16-O3	*1.265(4)*	*1.274(4)*	*1.272(6)*	*1.266(4)*
C18-O4	*1.264(3)*	*1.263(4)*	*1.270(6)*	*1.270(4)*
|ΔC-O|	*0.001(7)*	*0.011(8)*	*0.002(12)*	*0.004(8)*
C16-C17	*1.399(4)*	*1.397(5)*	*1.397(7)*	*1.393(5)*
C17-C18	*1.408(4)*	*1.410(5)*	*1.391(7)*	*1.391(5)*
|ΔC-C|	*0.009(8)*	*0.013(10)*	*0.006(14)*	*0.002(10)*
C31-O5	*1.260(4)*	*1.265(4)*	*1.262(6)*	*1.266(5)*
C33-O6	*1.266(3)*	*1.265(4)*	*1.272(6)*	*1.269(5)*

|ΔC-O|	*0.006(7)*	*0.000(8)*	*0.010(6)*	*0.003(10)*
C31-C32	*1.410(4)*	*1.397(5)*	*1.401(7)*	*1.406(5)*
C32-C33	*1.400(4)*	*1.403(5)*	*1.410(7)*	*1.396(5)*
|ΔC-C|	*0.010(8)*	*0.006(10)*	*0.009(14)*	*0.010(10)*
Mean |ΔC-O|, Å	***0.006(3)***	***0.005(4)***	***0.007(6)***	***0.005(4)***
Mean |ΔC-C|, Å	***0.009(4)***	***0.0070(45)***	***0.005(7)***	***0.011(5)***

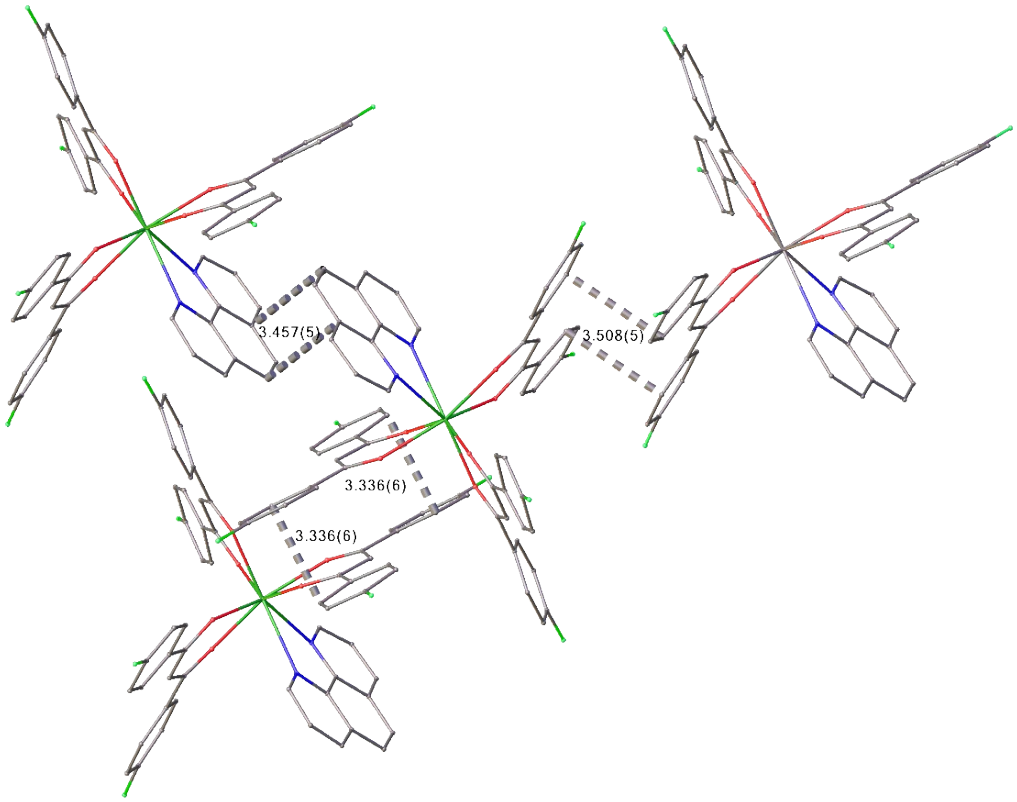

Figure S2. π...π interactions in ***Eu-FDBM-p***. All hydrogen atoms and thermal displacement ellipsoids are omitted for clarity, intermolecular π-stacking is shown with bold dashed lines, shortest C-C distance is illustrated.

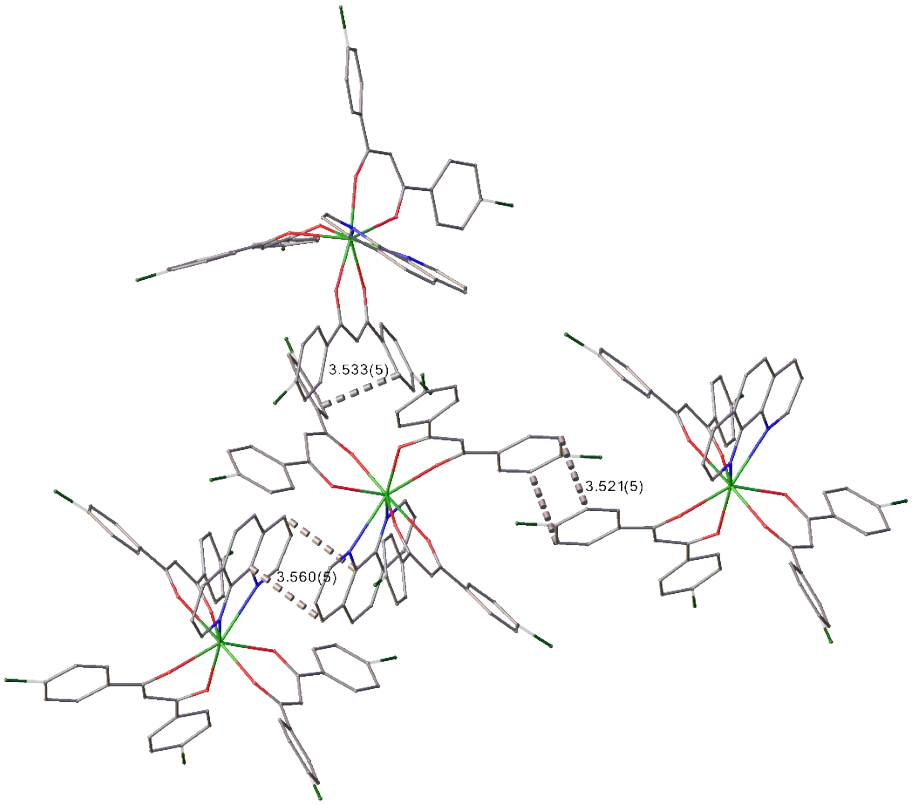

Figure S3. π...π interactions in ***Eu-ClDBM-p***. All hydrogen atoms and thermal displacement ellipsoids are omitted for clarity, intermolecular π-stacking is shown with bold dashed lines, shortest *C*-*C* distance is illustrated.

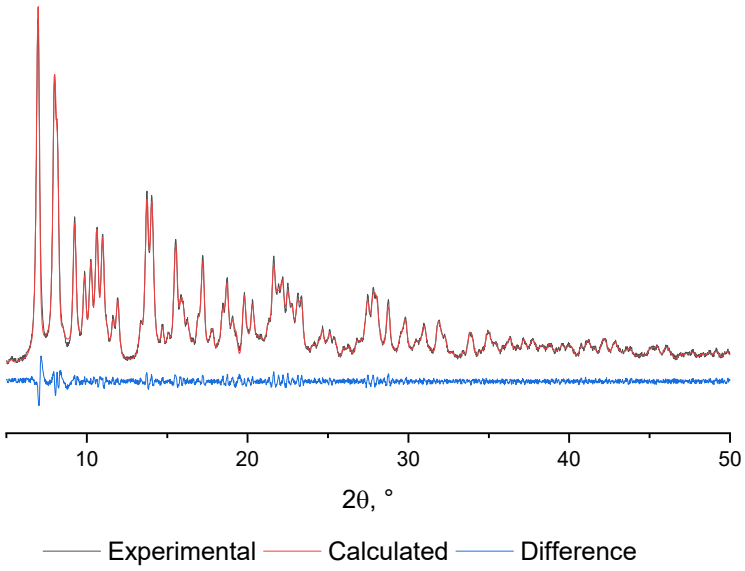

Figure S4. PXRD pattern of ***Eu-FDBM-p*** complex and simulated from single crystal data one.

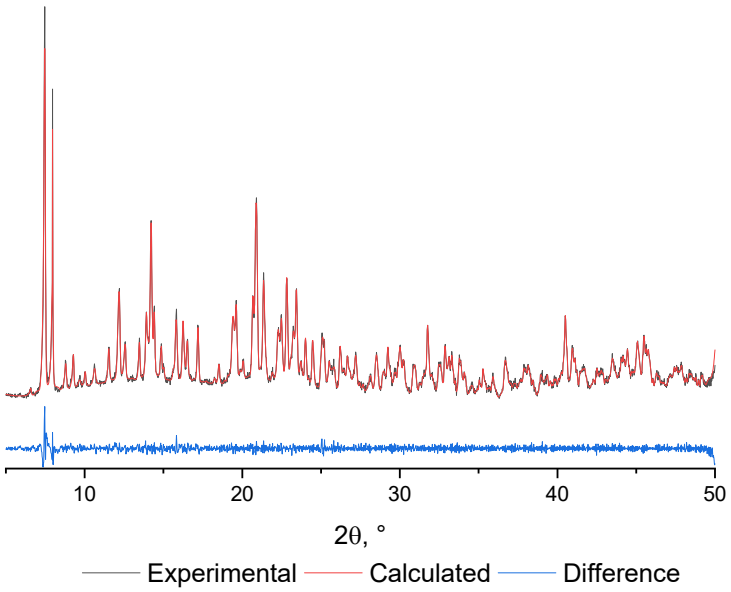

Figure S5. PXRD pattern of ***Eu-ClDBM-p*** complex and simulated from single crystal data one.

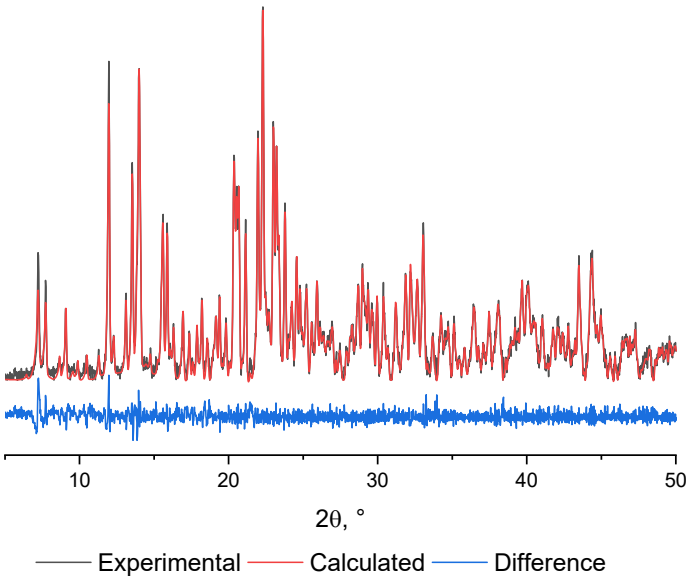

Figure S6. PXRD pattern of ***Eu-BrDBM-p*** complex and simulated from single crystal data one.

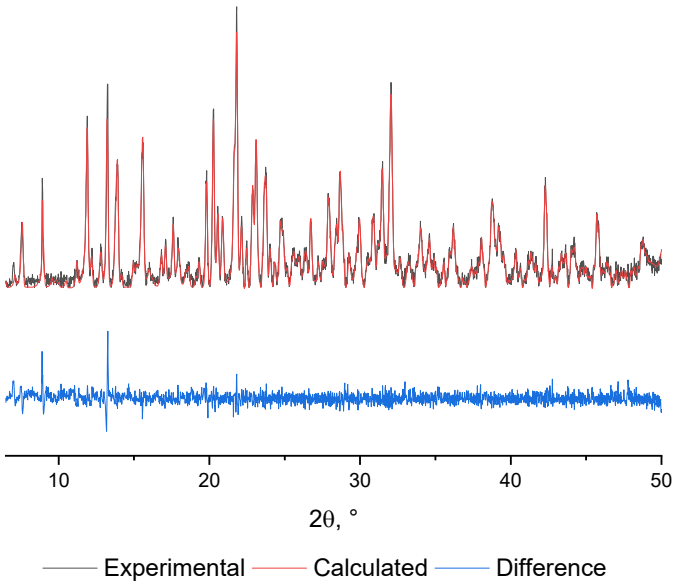

Figure S7. PXRD pattern of ***Eu-IDBM-p*** complex and simulated from single crystal data one.

SI-2.3. UV-Vis spectroscopy

UV-Vis spectra for THF solutions of the complexes and ***HIDBM, HBrDBM, HClDBM*** and ***HFDBM*** ligands are shown in Figure S8. The compounds intensively absorb emission in the spectral range of 250-400 nm. The absorption band located at ca. 350 nm is associated with electronic π-π^* transitions of β-diketone fragment.[30] The peaks at 270 and 293 nm correspond to *1,10*-phenanthroline. Since all the ***Eu-XDBM-p*** spectra qualitatively resemble each other (X=F, Cl, Br, I), the chemical binding of the investigated ligands to the Eu^{3+} ion does not significantly affect their β-diketone ligand energy structure. The investigated compounds exhibit high molar extinction ϵ by order of 10^4 $mol^{-1}cm^{-1}L$ contrary to low absorption of Eu^{3+} ion $\epsilon \approx 5$ L mol^{-1} cm^{-1}.[31] Moreover, halogenation of aromatic fragment in dibenzoylmethane ligand shifts the first excited singlet state energy of ligand in the coordination compounds from 24550 cm^{-1} up to 26300 cm^{-1} (see **Table S5**).

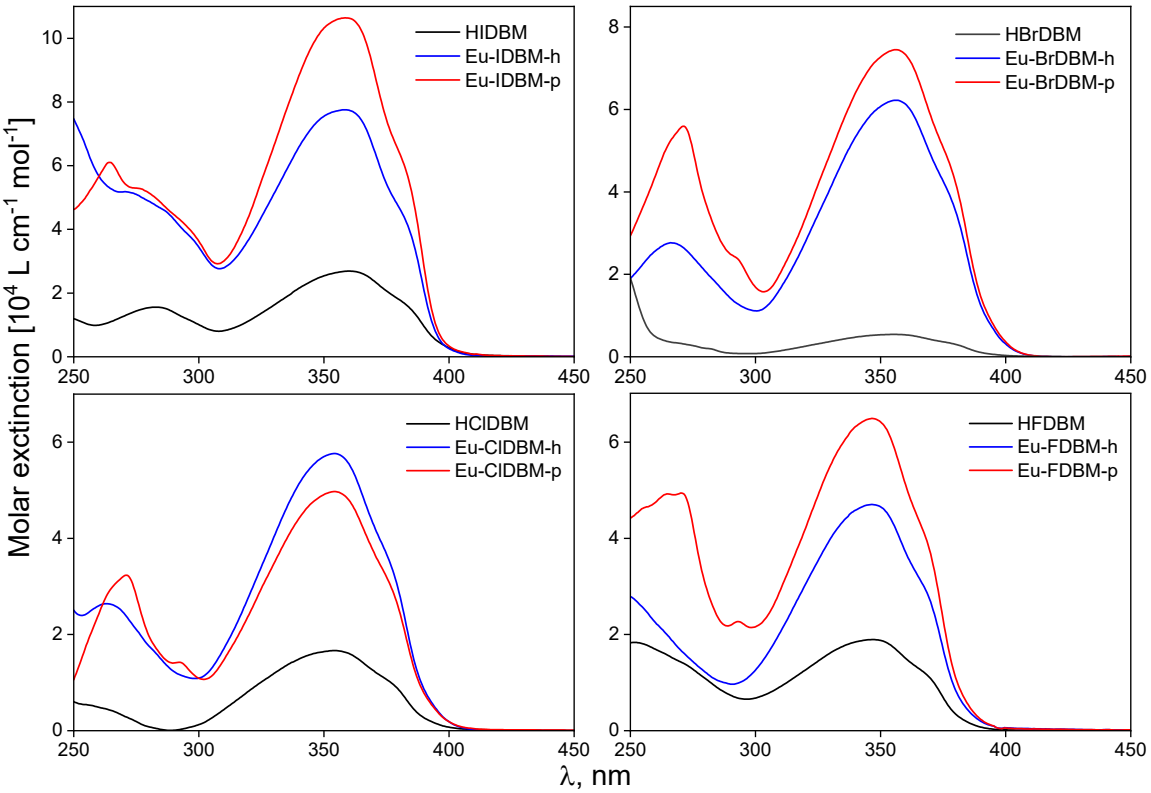

Figure S8. Optical absorption spectra for the investigated complexes and ***HIDBM***, ***HBrDBM***, ***HClDBM*** and ***HFDBM*** ligands dissolved in THF.

SI-2.4. Luminescence and excitation spectra

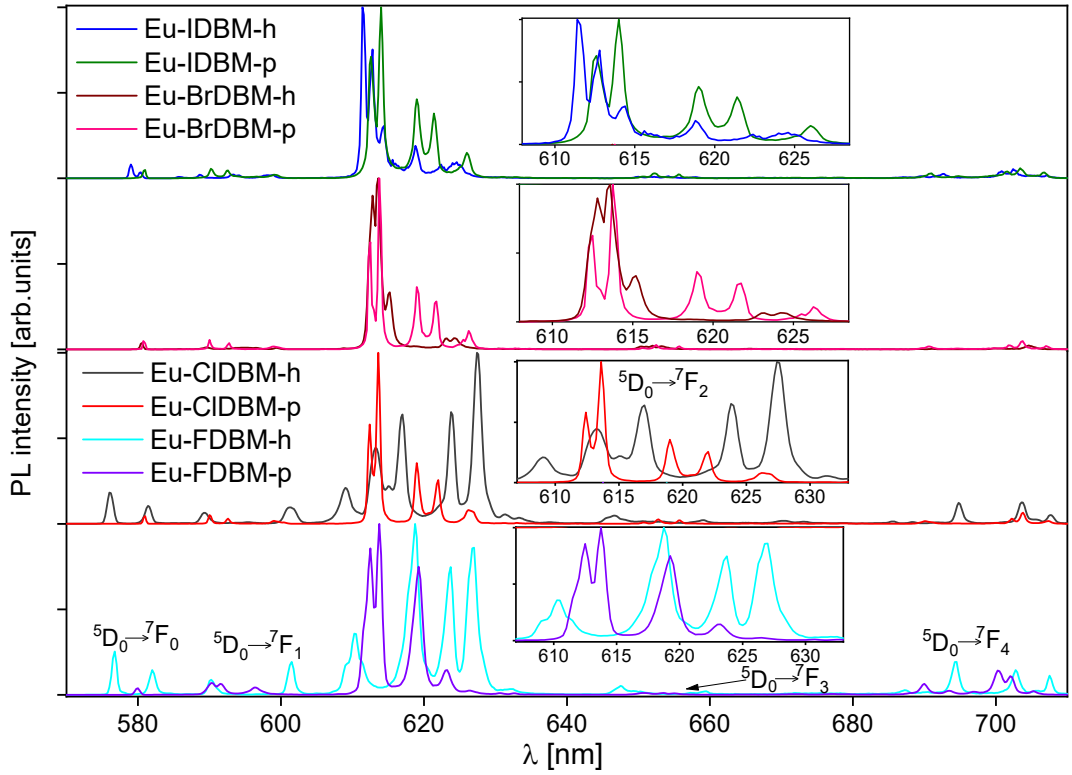

Figure S9. The luminescence spectra of ***Eu-IDBM-h, Eu-IDBM-p, Eu-BrDBM-h, Eu-BrDBM-p, Eu-ClDBM-h, Eu-ClDBM-p, Eu-FDBM-h, Eu-FDBM-p*** complexes in the crystalline phase upon excitation at 360 nm at 77 K.

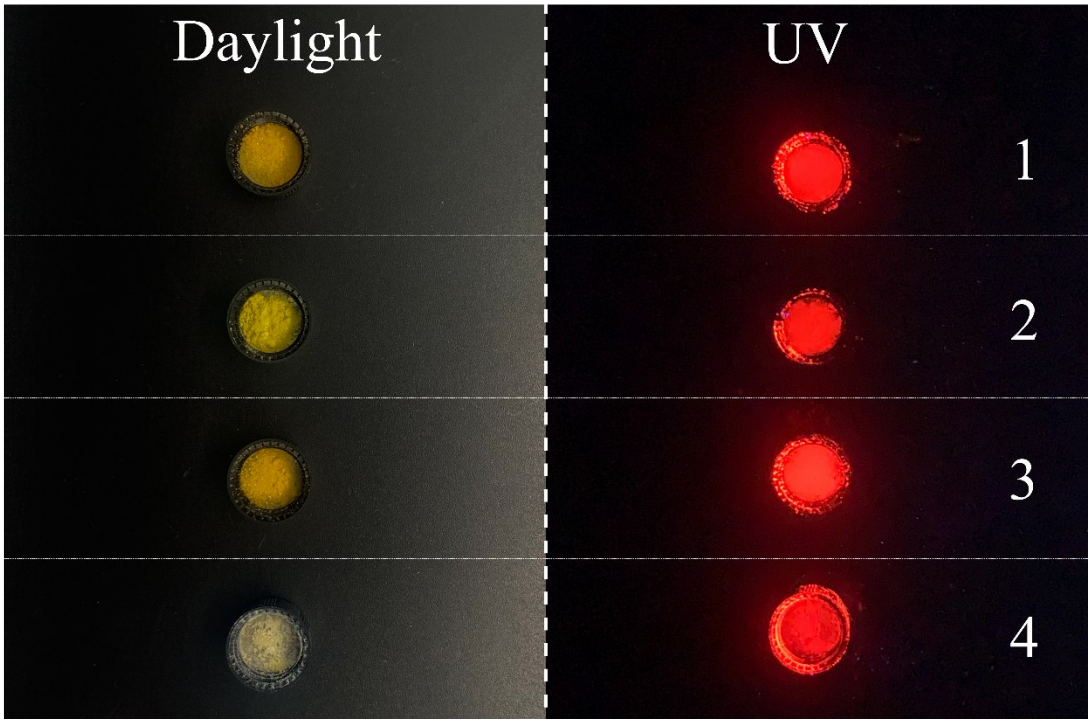

Figure S10. Crystal compounds under daylight and UV irradiation: 1 - ***Eu-IDBM-p***, 2 - ***Eu-BrDBM-p***, 3 - ***Eu-ClDBM-p*** and 4 - ***Eu-FDBM-p***.

Table S4. The energies in cm^{-1} of the Stark components for the f^*-f transitions in Eu^{3+} ion for the investigated compounds.

Parameter	Energy, cm^{-1}							
	Eu-IDBM-h	***Eu-IDBM-p***	***Eu-BrDBM-h***	***Eu-BrDBM-p***	***Eu-ClDBM-h***	***Eu-ClDBM-p***	***Eu-FDBM-h***	***Eu-FDBM-p***
$^5D_0 \rightarrow {}^7F_0$	17268 17229*	17211	17225	17219	17362 17200[a)]	17212	17339 17182*	17197
$^5D_0 \rightarrow {}^7F_1$	17071 16986 16856 16725	16942 16876 16692	16961 16918 16880 16841 16808 16762 16684	16949 16870 16696	16965 16797 16630	16946 16875 16693	16941 16863 16627	16897 16861 16725
$^5D_0 \rightarrow {}^7F_2$	16353 16318 16279 16233 16159 16067 16012	16323 16286 16154 16092 15973	16319 16299 16254 16049 16017	16329 16293 16154 16085 15987 15968	16418 16306 16257 16208 16027 15937 15840 15790	16329 16297 16154 16078 15963	16384 16167 16036 15958 15819	16404 16287 16253 16109 16009 15926 15819 15769
$^5D_0 \rightarrow {}^7F_3$	15384 15337 15198	15369 15331 15253	15376 15357 15308	15370 15326 15250	15466 15175 14920	15366 15319 15249	15443 15379 15164	15329 15268 15233
$^5D_0 \rightarrow {}^7F_4$	14555 14503 14436 14269 14236 14187 14141	14474 14392 14253 14217 14149	14959 14913 14512 14470 14285 14270 14192	14480 14396 14248 14211 14143	14587 14529 14457 14394 14210 14172 14130	14489 14396 14284 14240 14209 14137	14549 14484 14401 14228 14169 14134	14502 14463 14389 14317 14248 14214 14150

a) We denote the peaks to independent emission symmetry sites.

Table S5. The energies of S_1 and T_1 for free ligands and complexes.

Compound	Energy of S_1, ±100 cm^{-1}	Energy of T_1, ±100 cm^{-1}
HDBM	25500	-
HIDBM	25500	-
HBrDBM	26000	-
HClDBM	25500	-
HFDBM	26200	-
Gd(DBM)$_3$(H$_2$O)$_2$ [a)]	24550	20500

Gd-IDBM-h	25700	19800
Gd-BrDBM-h	25100	20600
Gd-ClDBM-h	26000	20300
Gd-FDBM-h	26300	19900

[a)]The experimental data for this compound were measured and described in our previous work.[32]

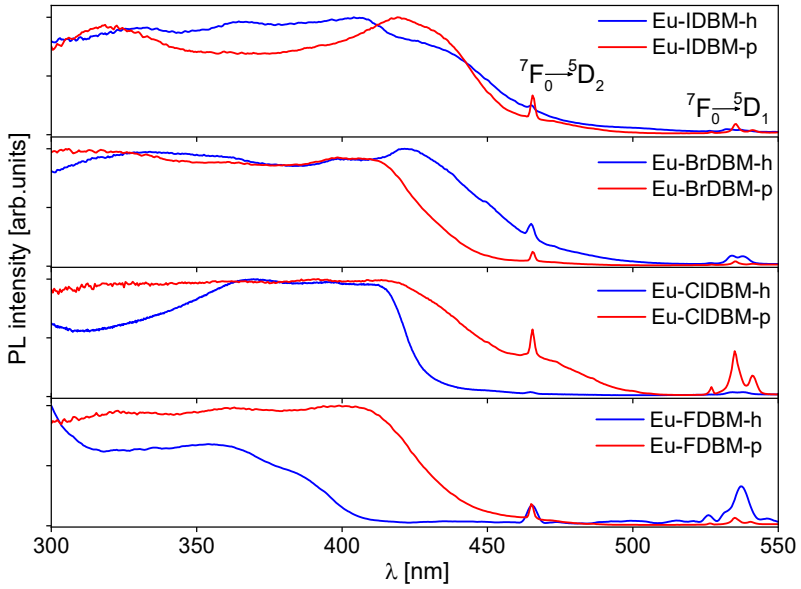

Figure S11. Optical excitation spectra of crystal complexes recorded at room temperature with registration at 615 nm.

SI-2.5. Energy of the first excited triplet state

To determine the energy of the first excited triplet level (T_1) of ligands ***IDBM, BrDBM, ClDBM*** and ***FDBM***, the Gd^{3+} complexes (***Gd-IDBM-h***, ***Gd-BrDBM-h, Gd-ClDBM-h*** and ***Gd-FDBM-h***, respectively) with the same ligand environments to ***Eu-IDBM-h***, ***Eu-BrDBM-h***, ***Eu-ClDBM-h*** and ***Eu-FDBM-h*** complexes were synthesized.

The position of the triplet levels of the most organic ligands, in particular β-diketones are below the resonant level of Gd^{3+} (energy of $^6P_{7/2}$ is 32000 cm^{-1}). It prevents direct energy transfer from the ligand to the Gd^{3+} ion. Therefore, the T_1 state undergoes radiative relaxation to the S_0 state. However, this transition is prohibited by the spin-selection rule that leads to a low emission intensity and relatively long lifetimes of the excited triplet state. Moreover, weak emission competes with non-radiative vibration relaxation of the T_1 state. Thus, in order to observe phosphorescence, complexes ***Gd-IDBM-h***, ***Gd-BrDBM-h, Gd-ClDBM-h*** and ***Gd-FDBM-h*** should be cooled to 77 K. Afterwards, the time-resolved luminescence spectra can be recorded to exclude the fluorescence from the emission spectrum.

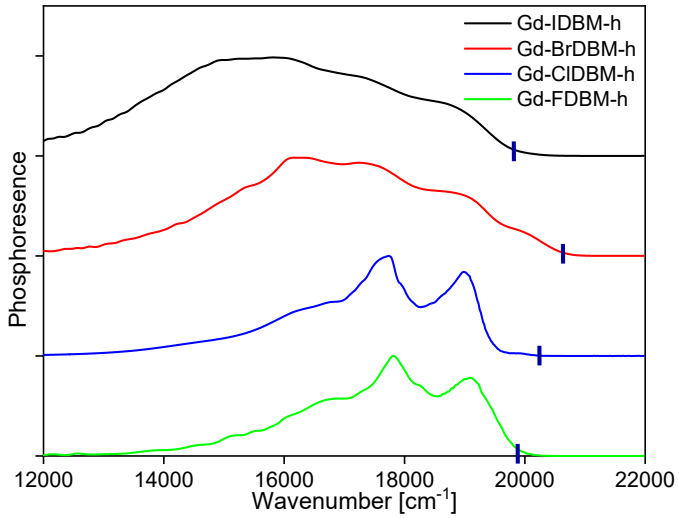

Figure S12. The phosphorescence spectra for ***Gd-IDBM-h***, ***Gd-BrDBM-h***, ***Gd-ClDBM-h*** and ***Gd-FDBM-h*** complexes in solid state measured at 77 K.

SI-2.6. Security Features Application

For more clear understanding of the anti-countering approach we estimated the emission intensities and the ratio of the emission intensities of the compounds utilized in the taggant with respect to the time of exposure (see Figures S13). The PL intensity decreases by 38 %, 27 %, 23 % and 8 % after 10 min continuous optical exposure at 360 nm (power density ~ 3.9 mW/cm^2) for ***Eu-IDBM-p***, ***Eu-BrDBM-p***, ***Eu-ClDBM-p*** and ***Eu-FDBM-p***, respectively (see Figure S13, left). As shown at the Figure S13 (right) the ratio of emission intensities rapidly increase during first 3 minutes of exposure. Within this time window the encryption is smoothly becomes more contrasting. Then, the time dependence of intensities ratio is nearly linear and after 5 minutes of exposure it almost reaches the plateau: the part of taggant is completely photobleached that supports our observations in the Figure 4.

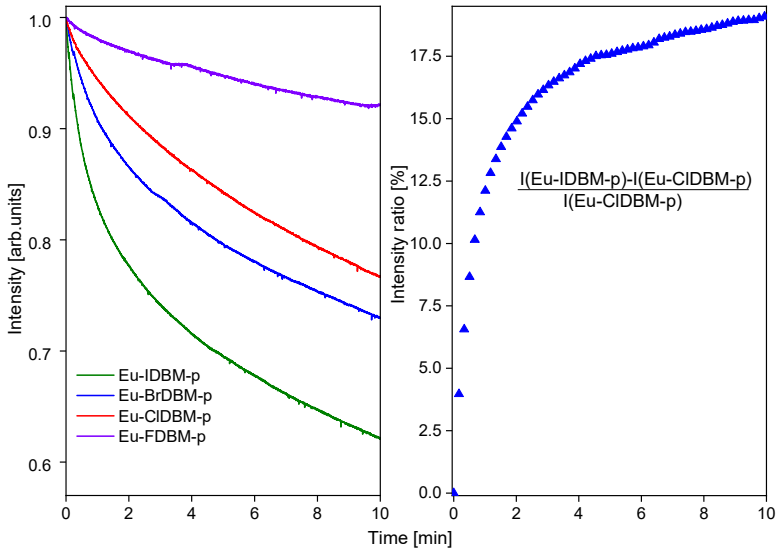

Figure S13. Left: PL intensity registered at 615 nm as function on time upon continuous excitation at 360 nm (power density ~ 3.9 mW/cm^2); Right: the ratio of the emission intensities of the compounds utilized in the taggant as the function of time exposure.

SI-2.7. PL decays and quantum yields

The hydrated compounds containing I, Cl and F heteroatoms have two peaks in this spectral range, so it can be concluded about two emission sites in ***Eu-IDBM-h, Eu-ClDBM-h*** and ***Eu-FDBM-h.*** The **Eu(DBM)$_3$(H$_2$O)$_2$** and **Eu(DBM)$_3$Phen** complexes also include two emission sites. However, the halogen substitution reduces splitting of energy transitions that indicates a decrease in the coordination polyhedron symmetry.

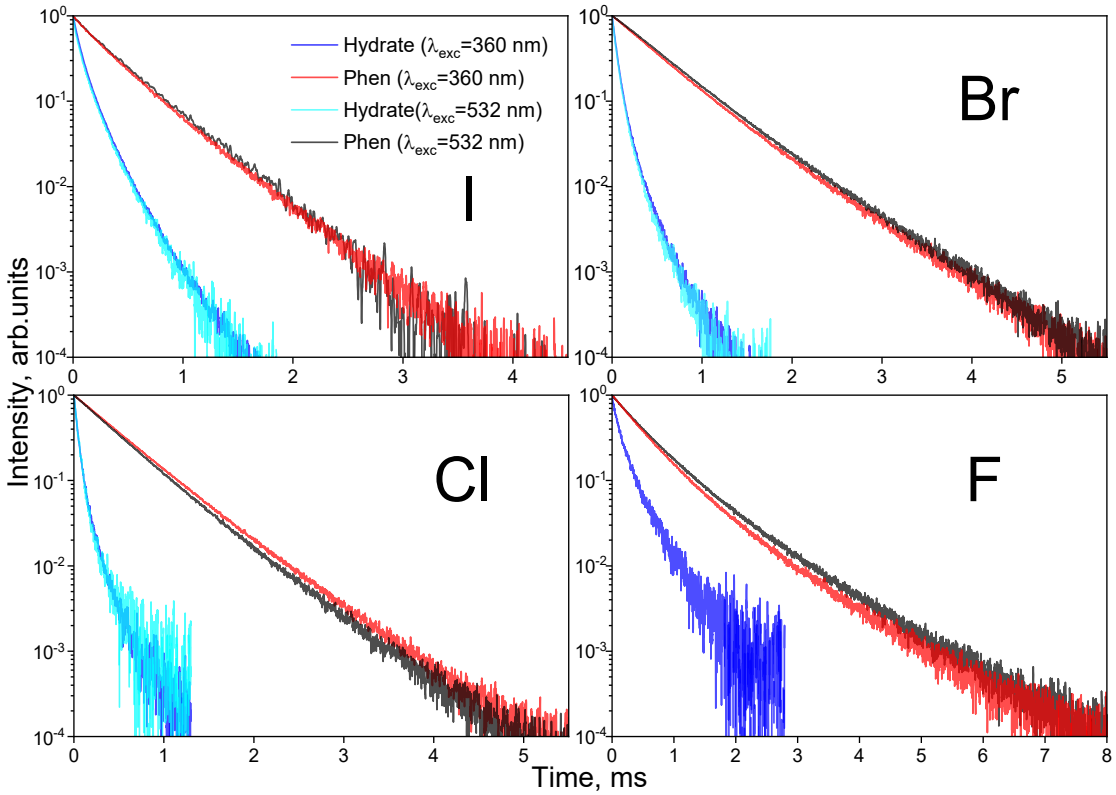

Figure S14. The photoluminescence decays for complexes in crystal powder in the visible spectral range at the room temperature excited directly through ion at 532 nm and through ligand environment (360 nm) and registered at 615 nm (red and black curves for compounds containing 1,10-phenantrolline ligand, light-blue and dark-blue curves for hydrated compounds).

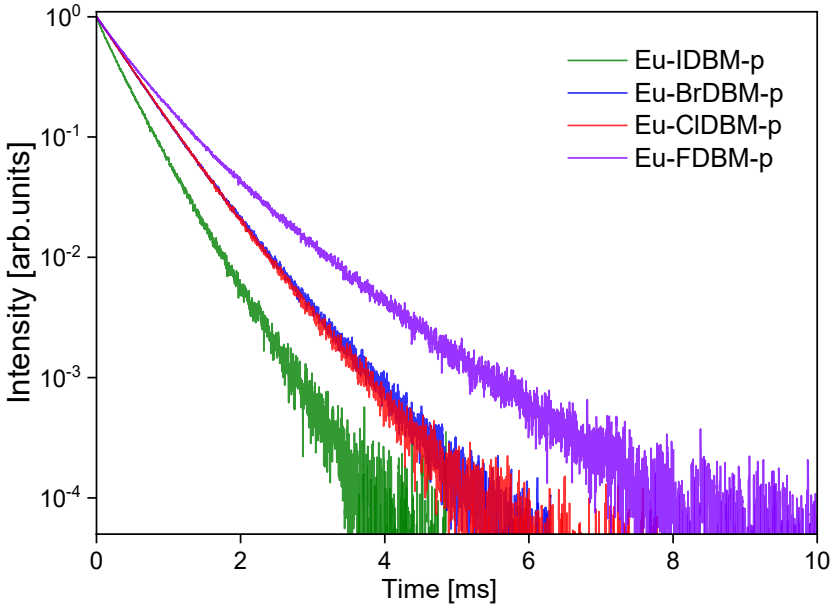

Figure S15. The PL decays for ***Eu-IDBM-p***, ***Eu-BrDBM-p***, ***Eu-ClDBM-p*** and ***Eu-FDBM-p*** complexes in crystalline powder at the room temperature upon excitation at 360 nm registered at 615 nm.

Luminescence decays obey a multi-exponential law

$$I(t) = A_1 e^{-\frac{t}{\tau_1}} + A_2 e^{-\frac{t}{\tau_2}}, \quad \textbf{(S1)}$$

where the observed lifetimes τ_1 and τ_2 in the experiment are defined as

$$\tau = \frac{1}{k} = \frac{1}{k_{rad} + k_{nrad}}, \quad \textbf{(S2)}$$

k_{rad} and k_{nrad} – the rate constants of radiative and non-radiative relaxation, respectively.

Table S6. Luminescence lifetimes for hydrated crystalline powder complexes at the room temperature.

Compound	λ_{exc}, nm	τ_1, μs	τ_2, μs	A_1	A_2	R^2
Eu-IDBM-h	360	54.2±0.2	153.1±0.4	0.62	0.37	0.999
	532	34.5±0.3	128.5±0.6	0.48	0.49	0.999
Eu-BrDBM-h	360	45.0±0.1	133.1±0.7	0.16	0.84	0.999
	532	48.0±0.5	135.3±1.5	0.76	0.22	0.997
Eu-ClDBM-h	360	35.6±0.1	112±1	0.81	0.18	0.999

	532	35.5±0.1	111±1	0.81	0.19	0.999
Eu-FDBM-h	360	74±1	267±2	0.52	0.44	0.998
	532	-	-	-	-	-

Table S7. Luminescence lifetimes for crystalline powder complexes containing 1,10-phenantrolline (300 K).

Compound	λ_{exc}, nm	τ_1, μs	τ_2, μs	A_1	A_2	R^2
Eu-IDBM-p	360	188.0±2.5	404.3±1.1	0.24	0.74	0.999
	532	101.0±4.3	399.9±1.0	0.14	0.86	0.999
Eu-BrDBM-p	360	446.4±0.6	650.0±1.0	0.76	0.25	0.999
	532	496.1±0.3	850.0±1.0	0.95	0.07	0.999
Eu-ClDBM-p	360	482.0±0.8	883.2±20.1	0.95	0.05	0.999
	532	452.2±0.9	777.3±17.7	0.93	0.07	0.999
Eu-FDBM-p	360	433.9±0.8	898.3±2.3	0.65	0.34	0.999
	532	429.9±0.7	892.6±3.0	0.76	0.25	0.999

The value of the internal quantum yield can be estimated by the following formula

$$\Phi_{Ln} = \frac{k_{rad}}{k_{rad} + k_{nrad}}. \quad \textbf{(S3)}$$

Since the rate constant of the magnetic-dipole transition ($^5D_0$-$^7F_1$) in Eu^{3+} k_{MD}=14.65 s^{-1} does not depend on the electric field induced by the ligand, it is possible to determine the value of k_{rad} by the relation

$$k_{rad} = k_{MD} n^3 \frac{I_{tot}}{I_{MD}}, \quad \textbf{(S4)}$$

where n = 1.5 – a refractive index, I_{tot}/I_{MD} – the ratio of the total integral luminescence intensity to the integral intensity of the magnetic-dipole transition. The constant k_{nrad} was evaluated using a simple dependency

$$k_{nrad} = \frac{1}{\tau} - k_{rad}, \quad \textbf{(S5)}$$

including the calculated k_{rad} and the observed lifetime τ is a weighted mean value calculated using τ_1 and τ_2, measured with resonant excitation of Eu^{3+} at the wavelength 532 nm.[33]

Table S8. Photophysical parameters for crystal powder complexes: k_{rad} and k_{nrad} – radiative and non-radiative processes rates, k_{BET} – the BET process rate, the internal quantum yield Φ_{Ln}, the overall Φ quantum yield and the sensitization efficiency η.

Compound	I_{tot}/I_{MD}	k_{rad}, s^{-1}	k_{nrad}, s^{-1}	k_{BET}, s^{-1}	τ^{-1}, s^{-1}	Φ_{Ln}, %	Φ, %	η
Eu-IDBM-h	26.3	1302.0	27683.5	-	28986	4.5	0.3	0.05
Eu-IDBM-p	23.1	1142.3	1553.097	528	2695.4	41.6	18.4	0.43
Eu-BrDBM-h	36.2	1787.6	22602.66	-	24390	7.3	0.4	0.05
Eu-BrDBM-p	22.3	1104.2	807.8	416	1912	56.3	30.9	0.54
Eu-ClDBM-h	30.7	1518.6	25729.3	-	27247	5.6	0.1	0.02
Eu-ClDBM-p	-	-	-	429	-	-	64.3	-
Eu-FDBM-p	16.7	824.6	1012.3	998±9	1836.9	44.9	41.1	0.92
[Eu(DBM)$_3$Phen][a)]	25.5	1262	1288	-	2550	49.5	23.3	0.47

[a)]The experimental data for this compound are taken from the work.[32]

SI-2.8. Energy transfer

The luminescence spectra of ***[Eu(DBM)$_3$Phen]*** and investigated complexes at 77 K (see Figure S16, a), fluorescence of corresponding free ligands at 300 K (see Figure S16, b) and the time-resolved emission spectra of ***[Gd(DBM)(H$_2$O)$_2$]***, ***Gd-IDBM-h, Gd-BrDBM-h, Gd-ClDBM-h and Gd-FDBM-h*** at 77 K (see Figure S16, c) were measured in solid state. All the spectra are normalized on the maximum of ligand fluorescence. The emission spectra of free ligands and the corresponding complexes qualitatively resemble each other in the spectral range of 400-530 nm (see curves *a* and *b* in Figure S16). It's worth noting that the ion-centered luminescence is observed from 520 to 570 nm for all the compounds. Comparing the emission spectra of Eu^{3+} compounds with the phosphorescence of Gd^{3+} compounds and free ligand fluorescence in 480-520 nm spectral region, we conclude that the ligand phosphorescence is not observed in the emission spectra of Eu^{3+} complexes. This conclusion indirectly indicates that the T_1 state does not participate in energy transfer. On the contrary, the ***[Eu(DBM)$_3$Phen]*** compound demonstrates a remarkable ligand phosphorescence in 480-520 nm spectral range. Thus, the halogen (Br, Cl and F) substitution in aromatic moiety of β-diketone ligand significantly changes the nature of the energy migration pathways – the ISC process block occurs.

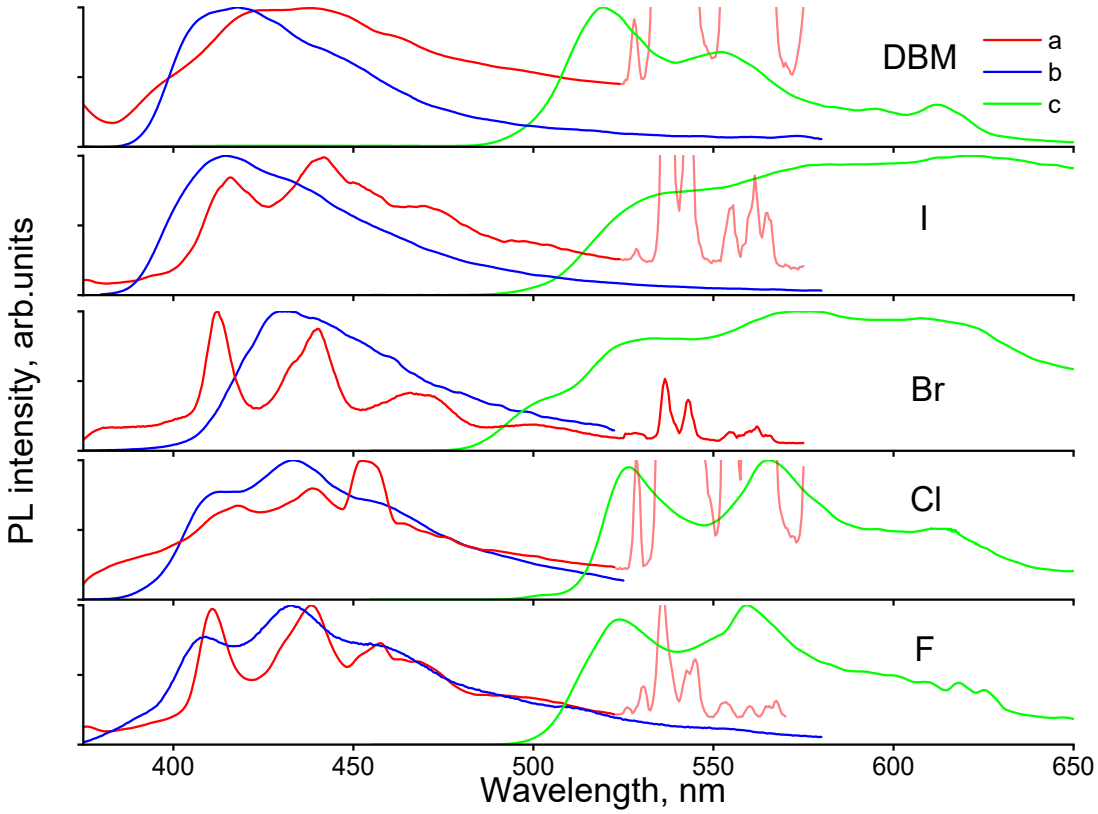

Figure S16. Photoluminescence spectra obtained for the compounds containing ***DBM***, ***IDBM***, ***BrDBM, ClDBM*** and ***FDBM*** ligands: a – emission of Eu compounds recorded at 77 K, b – fluorescence spectra of free ligands at 300 K, c – phosphorescence of Gd compound at 77 K.

SI-2.9. Back energy transfer process

The Arrhenius equation is given by

$$ln\left(\frac{1}{\tau_{300}}-\frac{1}{\tau_T}\right)=ln(k)=ln(A)-\frac{\Delta E_A}{R}T^{-1}, \quad \textbf{(S6)}$$

where τ_{300}, τ_T, R and T are an emission lifetime at 300 K, emission lifetime at T temperature, gas constant and compound temperature, respectively.

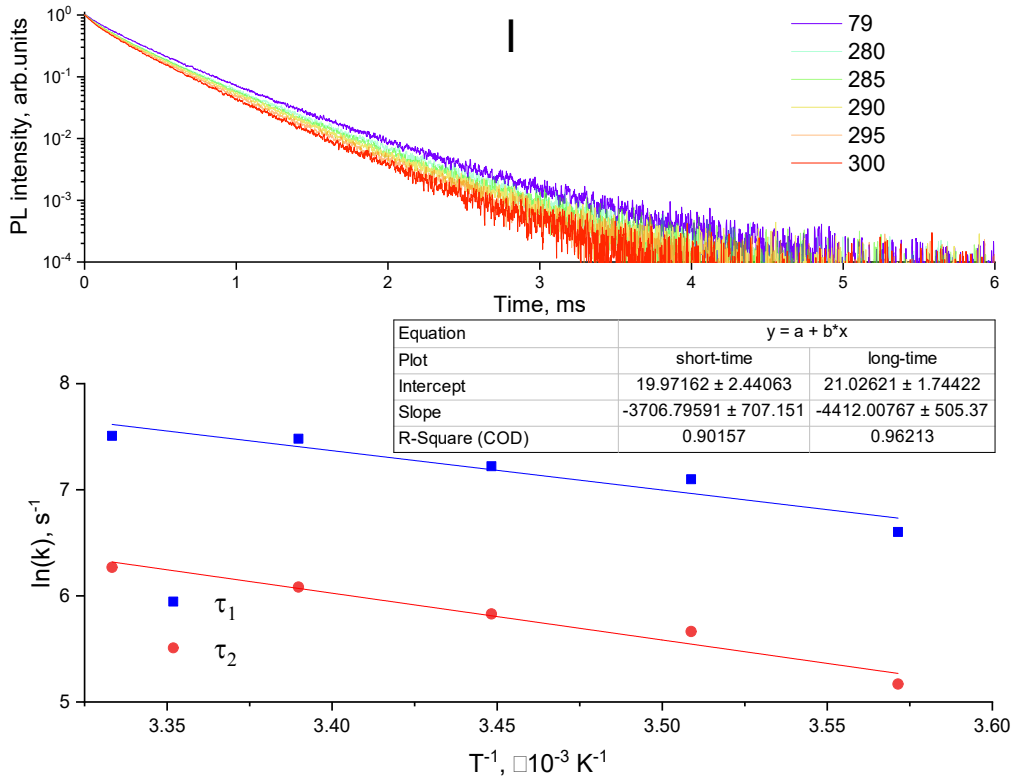

Figure S17. Temperature-dependent emission decays for ***Eu-IDBM-p*** compound in solid state at temperatures of 78-300 K under pulsed excitation at 360 nm.

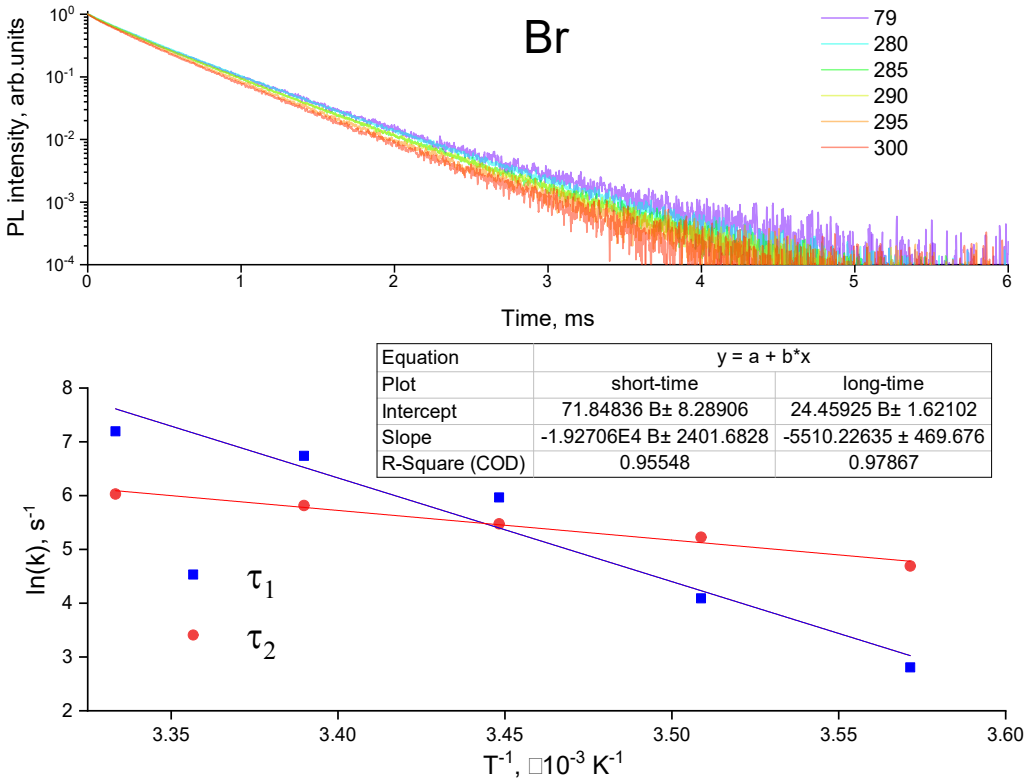

Figure S18. Temperature-dependent emission decays for ***Eu-BrDBM-p*** compound in solid state at temperatures of 78-300 K under pulsed excitation at 360 nm.

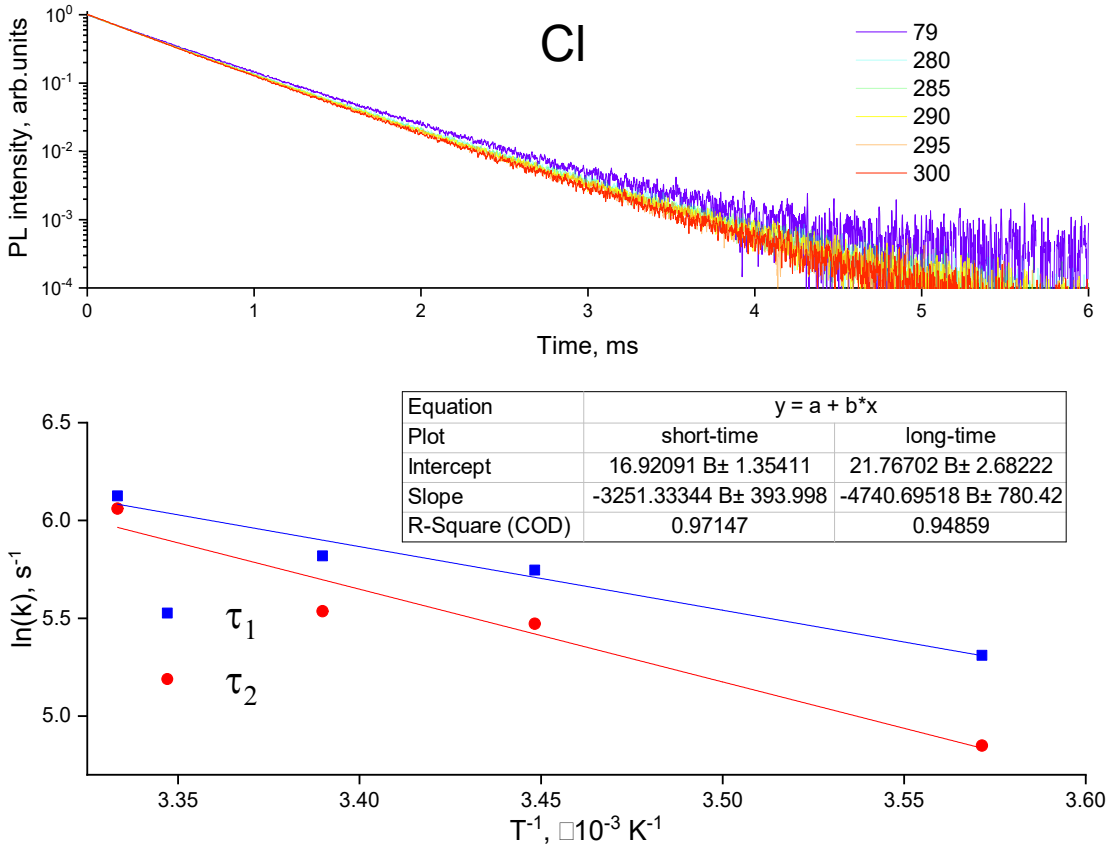

Figure S19. Temperature-dependent emission decays for ***Eu-ClDBM-p*** compound in solid state at temperatures of 78-300 K under pulsed excitation at 360 nm.

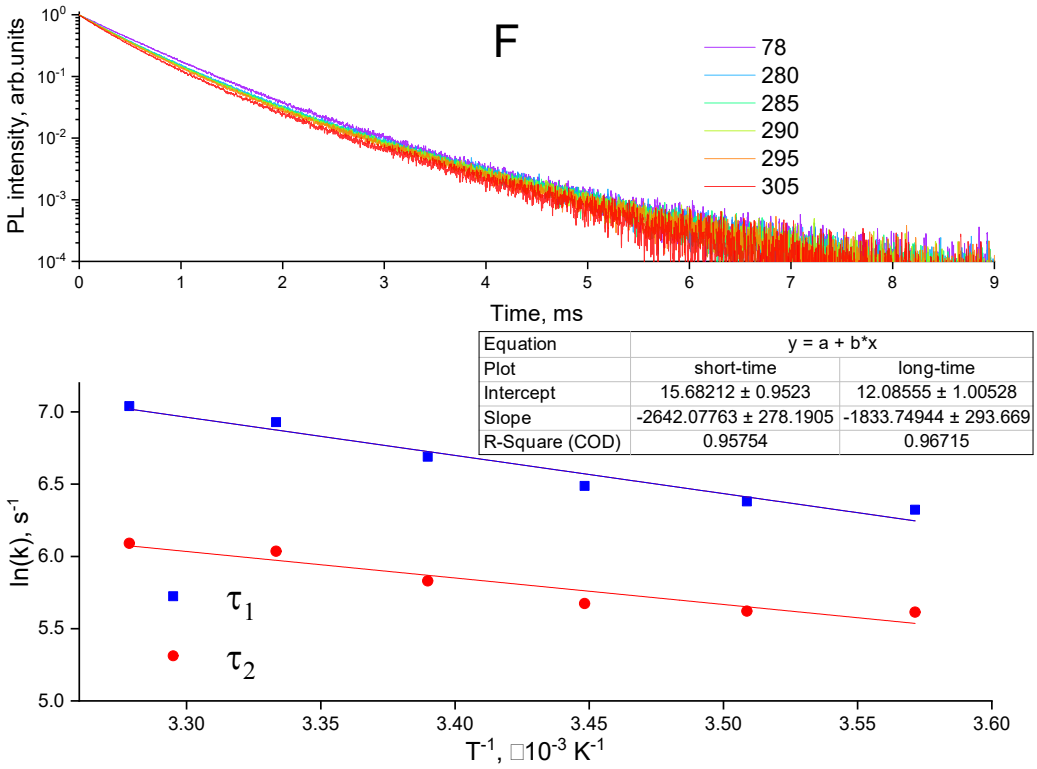

Figure S20. Temperature-dependent emission decays for ***Eu-FDBM-p*** compound in solid state at temperatures of 78-300 K under pulsed excitation at 360 nm.

Table S9. The luminescence lifetimes (τ_1 and τ_2) and corresponding amplitudes (A_1 and A_2) estimated from TSL experiment for ***Eu-IDBM-p*** compound.

T, K	τ_1, μs	τ_2, μs	A_1	A_2
79	225.36	488.91	0.45	0.52
280	193.32	450.22	0.37	0.54
285	177.1	428.47	0.36	0.59
290	172.28	419.13	0.36	0.57
295	161	402.59	0.34	0.58
300	159.83	388.58	0.34	0.57

Table S10. The luminescence lifetimes (τ_1 and τ_2) and corresponding amplitudes (A_1 and A_2) estimated from TSL experiment for ***Eu-BrDBM-p*** compound.

T, K	τ_1, μs	τ_2, μs	A_1	A_2
79	291.81	551.72	0.44	0.53
150	299.84	551.88	0.42	0.55

240	275.6	528.31	0.33	0.66
280	290.42	520.46	0.37	0.62
285	286.84	500.39	0.36	0.6
290	262	487.6	0.32	0.67
295	234.08	465.48	0.29	0.68
300	210.15	448.78	0.26	0.7

Table S11. The luminescence lifetimes (τ_1 and τ_2) and corresponding amplitudes (A_1 and A_2) estimated from TSL experiment for ***Eu-ClDBM-p*** compound.

T, K	τ_1, μs	τ_2, μs	A_1	A_2
79	473.4	777.3	0.83	0.16
280	446.43	671.6	0.75	0.24
285	425.64	619.59	0.63	0.37
290	425.48	625.25	0.67	0.33
295	422.65	616.13	0.67	0.34
300	393.55	573.37	0.54	0.48

Table S12. The luminescence lifetimes (τ_1 and τ_2) and corresponding amplitudes (A_1 and A_2) estimated from TSL experiment for ***Eu-FDBM-p*** compound.

T, K	τ_1, μs	τ_2, μs	A_1	A_2
78	519.4	1028	0.85	0.14
240	454.9	868.1	0.72	0.27
280	402.8	801.8	0.64	0.34
285	397.6	800.6	0.66	0.33
290	387.2	791.3	0.66	0.33
295	366.4	761.5	0.63	0.36
300	339.3	719	0.58	0.41
305	326.1	707	0.58	0.4

The process activation energy (ΔE_A) values were estimated by the Arrhenius equation for decay component with the highest probability (see **Table 3**). The sum of ΔE_A and $^5D_0$ state energies

for ***Eu-IDBM-p, Eu-BrDBM-p*** and ***Eu-ClDBM-p*** compounds is higher than the T_1 state energy by 200-500 cm^{-1} suggesting the BET process occurs from $^5D_0$ to T_1 state.[34] The obtained ΔE_A differs for ***Eu-IDBM-p, Eu-BrDBM-p*** and ***Eu-ClDBM-p*** and has the same trend with the T_1 state energy. We have established that the k_{BET} depends on the T_1 state energy of ligands. The $\Delta E_A = 1836$ cm^{-1} is the lowest for ***Eu-FDBM-p*** compound and approximately 2 times lower than the activation energy for other compounds. Moreover, the sum of ΔE_A and Eu^{3+} resonant state ($^5D_0$) energy is lower than the T_1 energy of the ligand and the parameter A is 10^3 times lower than that for other compounds. That implies that the T_1 state doesn't participate in the BET process for ***Eu-FDBM-p***. The BET process might occur to a charge transfer state, which is energetically lower that the T_1 state. As a result, the k_{BET} is 1.9 - 2.5 times higher for ***Eu-FDBM-p*** compound.

SI-2.10. Charge transfer states nature

As follows from section 2.3, all the investigated compounds exhibit bright ion-centered luminescence upon excitation in the spectral range of 400-500 nm that corresponds to some charge transfer (CT) states. In the present section, the nature of CT state is discussed in details. It is well-known that the charge transfer between the ligand and ion (LMCT) is not observed for Tb^{3+} coordination compounds, because the Tb^{3+} ion has a relatively high redox potential (E^o=3.1 V).[35] To check the presence of LMCT, the diffuse reflectance spectra for Eu^{3+} and Tb^{3+} compounds were recorded and compared pairwise (see Figure S21). The spectra are qualitatively the same for Eu^{3+} and Tb^{3+} compounds that proves the absence of the LMCT state.

The UV-vis spectra of ***Eu-ClDBM-p*** compound were measured in the $CHCl_3$, THF, DCM and DMSO solvents with different polarity (see Figure S22). The normalized UV-Vis spectra of the ***Eu-ClDBM-p*** compound in different solvents demonstrate absorption redistribution in the spectral range 300-420 nm. The central maximum shifts from 350 nm to 362 nm with the polarity increase. Moreover, an additional feature at ca. 400 nm appears for DCM and DMSO solutions. Since DCM and DMSO are more polar than $CHCl_3$ and THF, we conclude that this absorption band has the ILCT nature.[36]

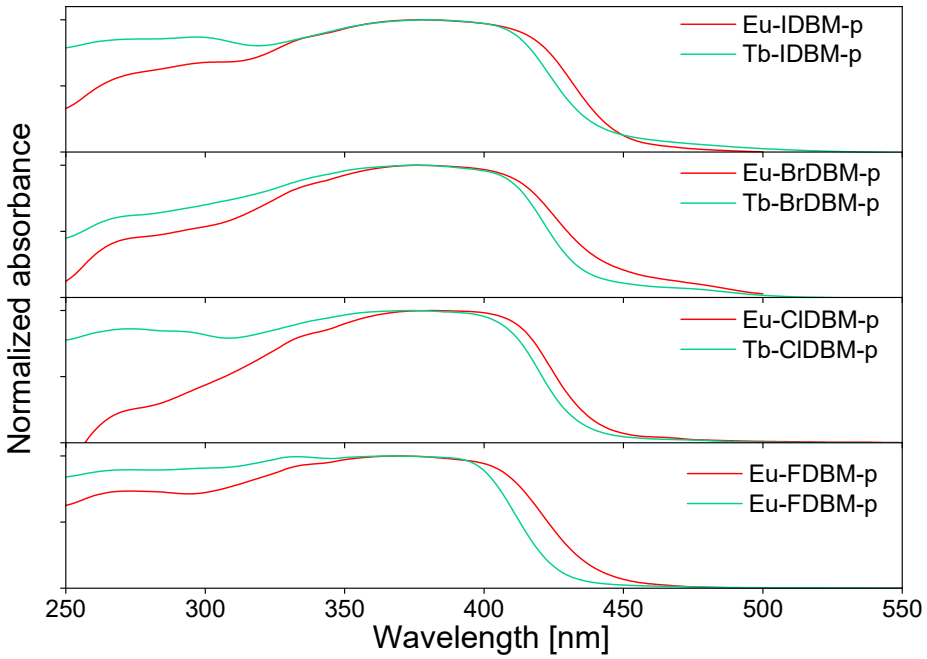

Figure S21. The diffuse reflectance spectra for Eu^{3+} and Tb^{3+} compounds.

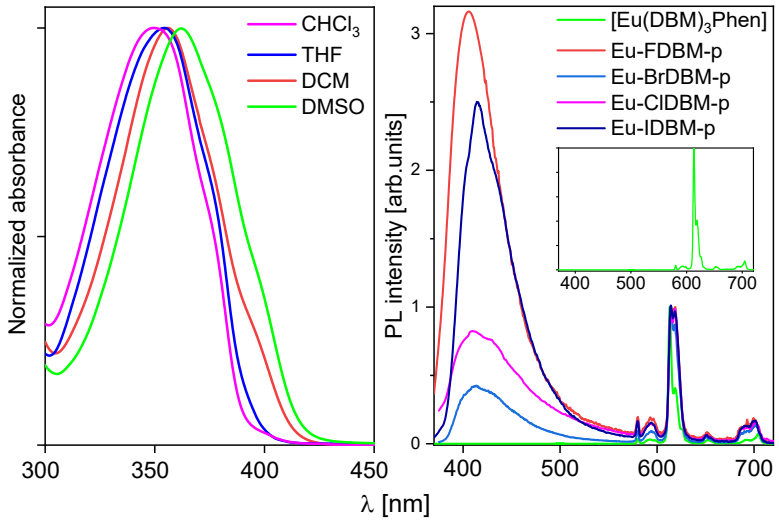

Figure S22. UV-Vis spectra for the ***Eu-ClDBM-p*** dissolved in $CHCl_3$, THF, DCM and DMSO (left). PL spectra for ***[Eu(DBM)$_3$Phen], Eu-IDBM-p, Eu-BrDBM-p***, ***Eu-ClDBM-p*** and ***Eu-FDBM-p*** compounds dissolved in THF upon CW excitation at 400 nm. The spectra are normalized on intensity of $^5D_0 \rightarrow {}^7F_2$ transition band.

SI-2.11. Electron scanning microscopy (SEM)

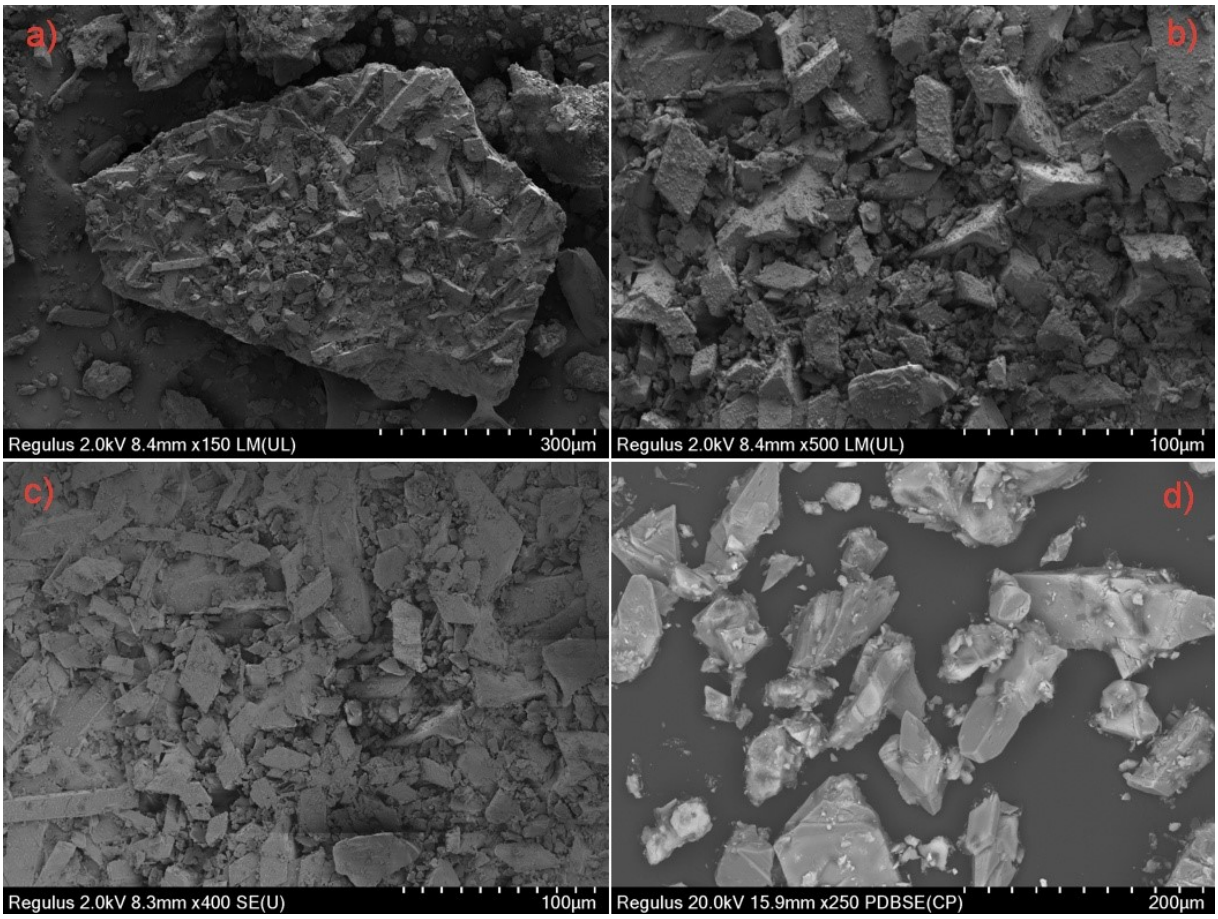

Figure S23. SEM images of ***Eu-FDBM-p*** (a), ***Eu-ClDBM-p*** (b), ***Eu-BrDBM-p*** (c) and ***Eu-IDBM-p*** (d).

References

[1] O. V. Dolomanov, L. J. Bourhis, R. J. Gildea, J. A. K. Howard, H. Puschmann, *J Appl Crystallogr* **2009**, *42*, 339.
[2] G. M. Sheldrick, *Acta Crystallogr C Struct Chem* **2015**, *71*, 3.
[3] V. V. Kachala, L. L. Khemchyan, A. S. Kashin, N. V. Orlov, A. A. Grachev, S. S. Zalesskiy, V. P. Ananikov, *Russ. Chem. Rev.*, **2013**, 82, pp. 648 - 685.
[4] A. S. Kashin, V. P. Ananikov, Russ. Chem. Bull. Int. Ed. **2011**, 60, pp. 2602 – 2607.
[5] C. Li, K. Xu, Z. Zhang, Macrocyclic and cage-like molecule and its derivative compound based on biphenyl aromatic hydrocarbon, its synthetic method and application. Patent application CN110642684 (15-10-2019). Chem. Abst. 2020:19204.
[6] D. Chiu, L. Chen, J. Yu. Narrow absorption polymer nanoparticles and related methods. Patent application WO2020060937 (16-09-2019). Chem. Abst. 2020:551625.
[7] Z. Liang, J. Song, R. He, Metal complex, polymer, mixture, composition, and organic electronic device. Patent application CN114369121 (15-10-2020). Chem. Abst. 2022:1003736.
[8] W. Keim, A. Behr, G. Kraus, *Journal of Organometallic Chemistry* **1983**, *251*, 377.
[9] C. Hassenrück, M. Azarkh, M. Drescher, M. Linseis, S. Demeshko, F. Meyer, R. F. Winter, *Organometallics* **2020**, *39*, 153.
[10] J. G. D. Elsberg, S. N. Anderson, D. L. Tierney, E. W. Reinheimer, L. M. Berreau, *Dalton Trans.* **2021**, *50*, 1712.
[11] P. Fries, M. K. Müller, J. Hartung, *Org. Biomol. Chem.* **2013**, *11*, 2630.

[12] K. C. Joshi, B. S. Joshi, *Synthesis and Reactivity in Inorganic and Metal-Organic Chemistry* **1986**, *16*, 1197.
[13] Kim, Hee Un, Lim, Jong Min, 황주현, 조남성, 이정익, Hwang, Don-Ha, *Bulletin of the Korean Chemical Society* **2013**, *34*, 399.
[14] K. Zhang, Z. Chen, Y. Zou, C. Yang, J. Qin, Y. Cao, *Organometallics* **2007**, *26*, 3699.
[15] P. C. Andrews, F. Hennersdorf, P. C. Junk, D. T. Thielemann, *Eur J Inorg Chem* **2014**, *2014*, 2849.
[16] A. O. Sarıoğlu, D. T. Kahraman, A. Köse, M. Sönmez, *Journal of Molecular Structure* **2022**, *1260*, 132786.
[17] H.-Y. Wong, W. Chan, G.-L. Law, *Molecules* **2019**, *24*, 662.
[18] A. O. Sarıoğlu, M. Sönmez, Ş. P. Yalçın, Ü. Ceylan, M. Aygün, *Journal of Coordination Chemistry* **2019**, *72*, 1108.
[19] J. J. Degnan, C. R. Hurt, N. Filipescu, *J. Chem. Soc., Dalton Trans.* **1972**, 1158.
[20] W. F. Sager, N. Filipescu, F. A. Serafin, *J. Phys. Chem.* **1965**, *69*, 1092.
[21] P. Lanoë, B. Mettra, Y. Y. Liao, N. Calin, A. D'Aléo, T. Namikawa, K. Kamada, F. Fages, C. Monnereau, C. Andraud, *ChemPhysChem* **2016**, *17*, 2128.
[22] G. E. Southard, G. M. Murray, *J. Org. Chem.* **2005**, *70*, 9036.
[23] P. K. Dhondi, P. Carberry, J. D. Chisholm, *Tetrahedron Letters* **2007**, *48*, 8743.
[24] R. Filler, Y. S. Rao, *J. Org. Chem.* **1971**, *36*, 1447.
[25] M. Lipp, F. Dallacker, S. Munnes, *Justus Liebigs Ann. Chem.* **1958**, *618*, 110.
[26] W. Franek, *Monatsh Chem* **1996**, *127*, 895.
[27] J. Qian, W. Yi, X. Huang, J. P. Jasinski, W. Zhang, *Adv Synth Catal* **2016**, *358*, 2811.
[28] R. G. Biswas, S. K. Ray, R. A. Unhale, V. K. Singh, *Org. Lett.* **2021**, *23*, 6504.
[29] K. Kumpan, A. Nathubhai, C. Zhang, P. J. Wood, M. D. Lloyd, A. S. Thompson, T. Haikarainen, L. Lehtiö, M. D. Threadgill, *Bioorganic & Medicinal Chemistry* **2015**, *23*, 3013.
[30] A. Ya. Freidzon, A. V. Scherbinin, A. A. Bagaturyants, M. V. Alfimov, *J. Phys. Chem. A* **2011**, *115*, 4565.
[31] K. Binnemans, *Coordination Chemistry Reviews* **2015**, *295*, 1.
[32] V. M. Korshunov, A. V. Tsorieva, V. E. Gontcharenko, S. R. Zanizdra, M. T. Metlin, T. A. Polikovskiy, I. V. Taydakov, *Inorganics* **2022**, *11*, 15.
[33] J.-C. G. Bünzli, S. V. Eliseeva, In *Lanthanide Luminescence* (Eds.: Hänninen, P.; Härmä, H.), Springer Berlin Heidelberg, Berlin, Heidelberg, **2010**, pp. 1–45.
[34] S. Omagari, In *Energy Transfer Processes in Polynuclear Lanthanide Complexes*, Springer Singapore, Singapore, **2019**, pp. 93–112.
[35] D. C. Harris, *Quantitative chemical analysis*, 7. ed., 2. print., Freeman, New York, **2007**.
[36] H. Kunkely, A. Vogler, *Inorganic Chemistry Communications* **1998**, *1*, 398.